Journal of Power Sources 195 (2010) 1059–1064

Contents lists available at ScienceDirect

Journal of Power Sources

journal homepage: www.elsevier.com/locate/jpowsour

Short communication

Chemical diffusivity and ionic conductivity of $GdBaCo_2O_{5+\delta}$

M.-B. Choi[a], S.-Y. Jeon[a], J.-S. Lee[a], H.-J. Hwang[b], S.-J. Song[a,*]

[a] Department of Materials Science and Engineering, Chonnam National University, 300 Yongbong-dong, Buk-gu, Gwangju 500-757, Republic of Korea
[b] Department of Materials Science and Engineering, Inha Univerity, 253 Yonghyun-dong, Nam-gu, Incheon 402-751, Republic of Korea

ARTICLE INFO

Article history:
Received 23 July 2009
Received in revised form 13 August 2009
Accepted 21 August 2009
Available online 2 September 2009

Keywords:
Ionic conductivity
Layered perovskite
Chemical diffusivity,
Intermediate-temperature solid oxide fuel cell

ABSTRACT

The transport properties of layered perovskite $GdBaCo_2O_{5+\delta}$ (GBCO), which has recently been proposed as a cathode material for intermediate-temperature solid oxide fuel cells (IT-SOFCs), are investigated as a function of oxygen partial pressure (OPP) over the oxygen partial pressure range of $10^{-4} \leq pO_2\,(atm) \leq 0.21$ at $1073 \leq T(K) \leq 1323$. The increase in total conductivity with increasing temperature below the low-temperature, order–disorder transition indicates a semiconductor-type behaviour with an activation energy of 0.42 eV. When OPP is increased to air pressure at a fixed temperature, the total conductivity increases with an apparent slope $(\partial \log \sigma / \partial \log pO_2)$ of 1/10 to 1/22. The maximum oxygen ion conductivity, as extracted from the oxygen permeation measurements, is around 0.01 S cm^{-1} under the nitrogen condition, which strongly supports the potential for cathode application. The chemical diffusion coefficient ($\tilde{D}$) and surface exchange coefficient (κ) are also calculated from the d.c. conductivity relaxation measurement and the values are best fitted by the following two equations:

$$\tilde{D}\ (cm^2\,s^{-1}) = 1.88 \times 10^{-2} \exp\left(-\frac{0.77\,eV}{kT}\right), \quad \kappa\ (cm\,s^{-1}) = 1.37 \times 10^{0} \exp\left(-\frac{0.86\,eV}{kT}\right)$$

1. Introduction

Fast oxygen ion conducting, double-layered perovskites have recently received considerable research attention because of their potential application in solid-state electrochemical devices, such as cathode materials for intermediate-temperature solid oxide fuel cells (IT-SOFCs), and oxygen separation membranes [1–3]. Particularly at low-temperatures, the experimental and theoretical results for the mixed conducting property of $GdBaCo_2O_{5+\delta}$ (GBCO) support its attractiveness as a material for IT-SOFCs because the decrease in the required operating temperature of SOFCs reduces the cost and enhances the material compatibility. Several studies have examined various properties of GBCO, such as total conductivity [4], oxygen diffusion [5], structural analysis [6], and non-stoichiometry with thermogravimetric analysis (TGA) [7]. The very high electric conductivity with increasing temperature was attributed to the charge disproportionation of $Co^{3+} \rightarrow Co^{2+} + Co^{4+}$ [8]. It was also reported that the GBCO showed excellent stability in air (<600 ppm CO_2) for long periods of time (100 h) at intermediate temperatures (500–700 °C) [9]. The chemical stability of GBCO has been studied with different oxide-ion conductors, e.g., 8 mol% Y_2O_3–ZrO_2, $La_{0.8}Sr_{0.2}Ga_{0.8}Mg_{0.2}O_{3-\delta}$, $Ce_{0.9}Gd_{0.1}O_{2-\delta}$ [9].

Protonic ceramic membrane fuel cells with layered GBCO cathode were also evaluated. GBCO was found to be a good cathode candidate for operating at or below 700 °C with a simple and potentially commercial method of manufacture, such as gel-casting or suspension spray [10].

The oxygen transport properties with respect to temperature and oxygen partial pressure (OPP) remain incompletely understood because of the difficulty in identifying the contribution of the oxygen ion conductivity to the measured total conductivity. Oxygen ionic conduction measurements are difficult due to the low ionic transport number of GBCO. Furthermore, even though oxygen transport kinetics are an important parameter in understanding the defect chemistry and optimizing SOFC performance, very few reports have attempted such optimization.

This study aims to determine the chemical diffusion coefficient and surface reaction rate constant in a N_2–O_2 atmosphere and the oxygen ion conductivity from oxygen permeation measurements to clarify both the mixed conductivity of GBCO and the effect of OPP on the transport kinetics. The thermal expansion coefficient, a basic physical property which can be of considerable importance in SOFC design is measured to confirm the phase transition from thermogravimetric/differential thermal analysis (TG/DTA) measurements.

* Corresponding author at: School of Materials Science and Engineering, Chonnam National University, 300 Yongbong-dong, Buk-gu, Gwangju 500-757, Republic of Korea. Tel.: +82 62 530 1706; fax: +82 62 530 1699.
E-mail address: song@chonnam.ac.kr (S.-J. Song).

0378-7753/$ – see front matter © 2009 Elsevier B.V. All rights reserved.
doi:10.1016/j.jpowsour.2009.08.074

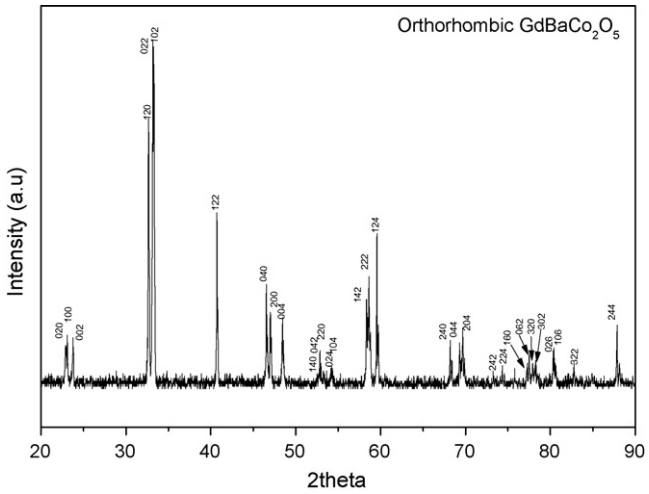

Fig. 1. Room temperature X-ray diffraction patterns of $GdBaCo_2O_{5+\delta}$ calcined at 1273 K in air.

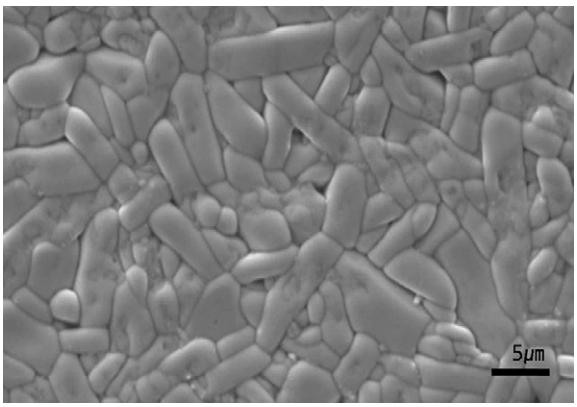

Fig. 2. Thermally etched surface microstructure image of $GdBaCo_2O_{5+\delta}$ sintered at 1430 K in air.

2. Experimental

Layered perovskite GBCO powders were prepared by a conventional solid-state reaction method. The starting materials of Gd_2O_3 (Aldrich, 99.99%), $BaCO_3$ (Aldrich, 99.99%), and Co_3O_4 (Aldrich, 99.9%) were weighed in the stoichiometric proportions of GBCO. The powders were mixed, ground in a ball mill with stabilized zirconia balls, and calcined at 1273 K for 24 h in air. The calcined oxide powders were then crushed, sieved to <45 μm, pressed into pellets, cold-isostatic-pressed, and sintered at 1430 K for 10 min in a microwave furnace for oxygen permeation measurements. The densities of the resultant discs are 96% of the theoretical values. As shown in Fig. 1, X-ray diffraction spectra confirm the attainment of single-phase orthorhombic GBCO (space group, *Pmmm*) via a microwave sintering procedure, in agreement with previous reports [3,11]. The specimens for d.c. conductivity relaxation measurements were cut out of the sintered disc in the form of an elongated, parallelepiped shape with dimensions of 1.94 mm × 1.94 mm × 16.71 mm [3].

The TG/DTA was performed with a SDT Q600 V8.0 Build 95 thermal analyzer at a heating rate of 10 °C min^{-1} from room temperature to 1173 K in air at a 100 cm^3 min^{-1} flow rate.

The total d.c. conductivity was measured by a standard, four-probe method using a measurement system that included a digital multimeter (Keithley 2700) combined with a programmable current source (Keithley 220). For d.c. relaxation measurements, a specimen was completely equilibrated in a given thermodynamic condition and then the oxygen chemical potential was abruptly changed to a different value while recording the electrical conductivity of the specimen with time until a new equilibrium was reached. In order to maintain a constant chemical diffusivity, a sufficiently small change of OPP was chosen. The overall measurements were repeated over the OPP range of $10^{-4} \leq pO_2\,(atm) \leq 0.21$ at $1073 \leq T\,(K) \leq 1323$. Thermal expansion was measured using a Netzch L75 PT1600 dilatometer from room temperature to 1273 K at 2 °C min^{-1} with an air purge at a flow rate of 50 cm^3 min^{-1}.

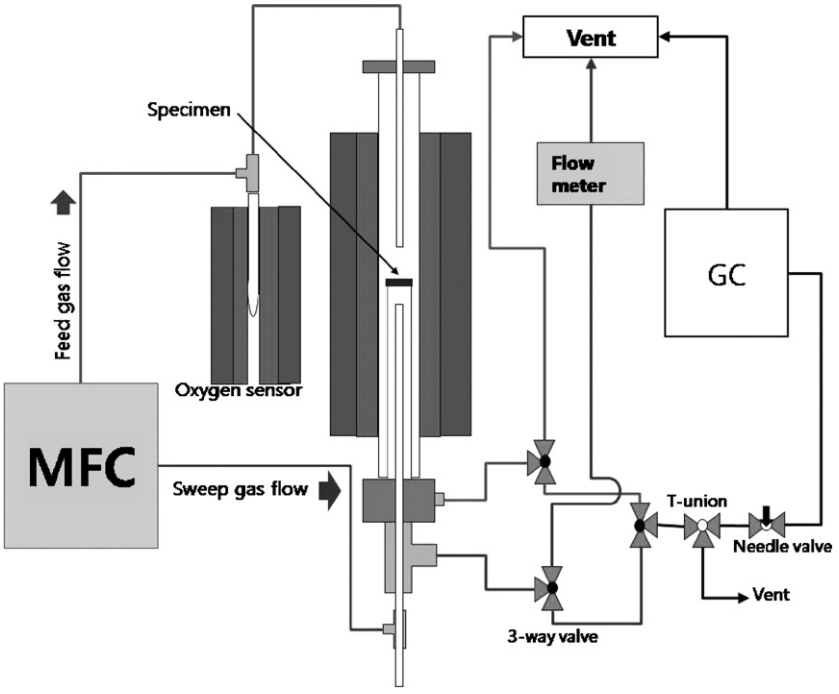

Fig. 3. Schematic of oxygen permeation measurements.

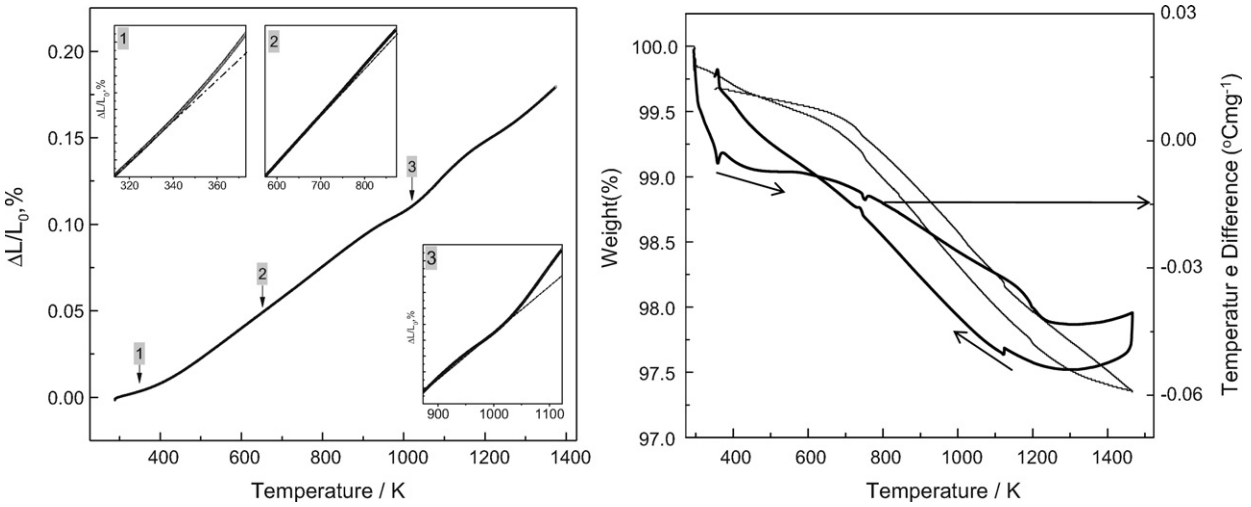

Fig. 4. (a) Thermal expansion curve for $GdBaCo_2O_{5+\delta}$ over temperature range of 303–1173 K and (b) TG/DTA curve for $GdBaCo_2O_{5+\delta}$ showing reversible structural transitions.

The oxygen permeation was measured using dense discs (≈96% of theoretical density, 13 mm in diameter, 1.14 mm thick). A scanning electron micrograph (SEM; Shimadzu, SS-550) image of the as-sintered surface, Fig. 2, shows well-developed grains and low porosity. The planar surface of each disc was polished with 600-grit SiC paper and then fixed to an alumina tube, as shown in Fig. 3. A seal was formed when the assembly was heated to 1233 K and spring-loaded rods were used to squeeze a gold ring between the membrane and the alumina tube. The sweep-side flow consisted of ultra-high purity helium at a constant flow rate of 100 sccm, while the feed gas flow consisted of an air/N_2 mixture at a flow rate of 100 sccm. The sweep gas flow during permeation measurements was controlled with a mass flow controller and the rate was measured with a flow calibrator (Digital flowmeter, Optiflow 570). The oxygen content of the permeate stream was measured with a gas chromatograph (Agilent 6890N) equipped with a TC detector. Any gas leakage through pores in the sample or through an incomplete seal was checked by measuring the N_2 content of the permeate stream. Data were collected only when the leakage rate was less than 1%. From the oxygen content measured on the sweep-side of the permeation assembly and the sweep gas flow rate, the total oxygen permeation rate was calculated for ideal gas behaviour. Then the permeation flux was calculated by dividing the permeation rates by the flat surface area of the disc membrane. In order to minimize edge contribution to the permeation, the membrane edge was sealed with a ceramic sealant.

3. Results and discussion

The thermal expansion curve of GBCO increases linearly with temperature between 303 and 1373 K, as seen in Fig. 4a. Three inflexions are revealed at about 373, 673, and 1073 K, and are respectively attributed to order–disorder transitions, as reported in a previous study [4], a phase transition from orthorhombic *Pmmm* to tetragonal *P*4/*mmm* [4], and thermally induced loss of lattice oxygen and the formation of oxygen vacancies due to cobalt cation reduction from Co^{4+} to Co^{3+} for charge neutrality [12]. A further inflexion around 1273 K is also present, but cannot be matched with any reported, structure analysis. The average thermal expansion coefficient is about $13 \times 10^{-6}\,K^{-1}$ between 303 and 1373 K in air. The trend thermal expansion trends agreed well with the results from thermal gravimetric analysis and differential thermal analysis of the GBCO powders, as shown in Fig. 4b. The hysteresis in the cooling and heating processes demonstrates the reversibility of the oxygen uptake process, along with the phase transition.

The transient total conductivity of GBCO was measured with increasing temperature at a ramp rate of 2 °C min^{-1} and the value of the equilibrium total conductivity was also collected from each of the conductivity relaxation profiles, as shown in Fig. 5. The total conductivity increases with increasing temperature below the low-temperature order–disorder transition (373 K), thereby indicating semiconductor-type behaviour with an activation energy of 0.42 eV, consistent with Ref. [11]. Note that this value differs substantially with the reported value in Ref. [4]. The reason for this difference is not clear at this point. Above the phase transition from orthorhombic *Pmmm* to tetragonal *P*4/*mmm*, the total conductivity decreases with increasing temperature, in line with the metallic behaviour reported in other studies [2,4].

The equilibrium total conductivities as a function of OPP at different temperatures are shown in Fig. 6a. When the OPP is increased to the value in air at a fixed temperature, the total conductivities increase with an apparent slope ($\partial \log \sigma / \partial \log pO_2$) of 1/10 to 1/22. Such behaviour has been generally observed in p-type conductors and is attributed to the generation of electron holes from the exter-

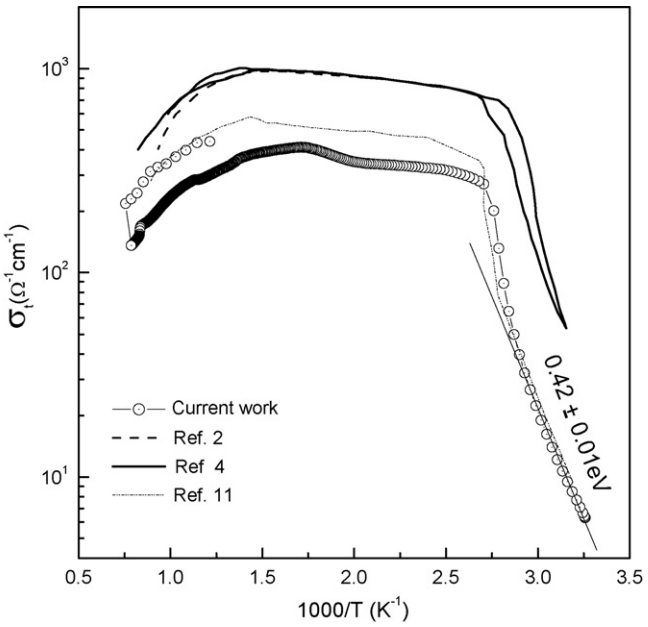

Fig. 5. Total conductivity of $GdBaCo_2O_{5+\delta}$ as function of temperature measured by four-probe d.c. conductivity method.

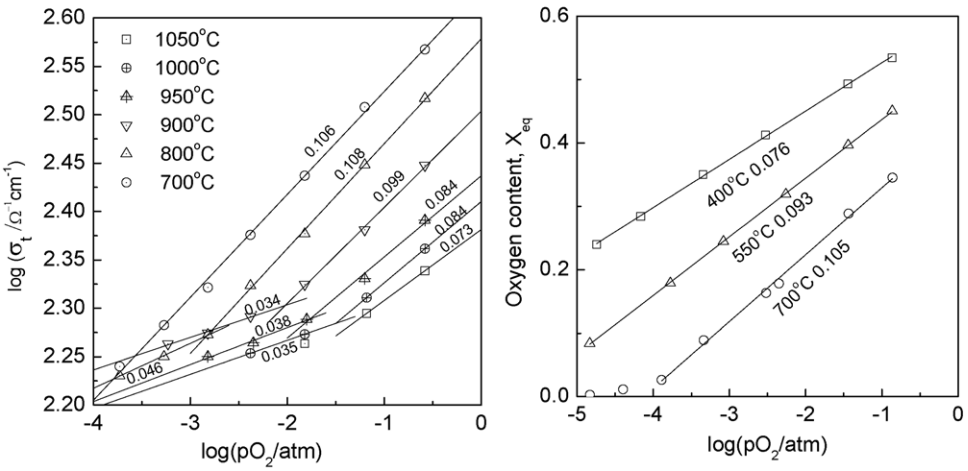

Fig. 6. (a) Total conductivity of $GdBaCo_2O_{5+\delta}$ as function of oxygen partial pressure (OPP) measured by four-probe d.c. conductivity method, and (b) dependence of equilibrium oxygen content on oxygen partial pressure for $GdBaCo_2O_{5+\delta}$ at reference [5].

nal reaction with the atmosphere, as described in Eqs. (1) and (2) with Kroger and Vink notations:

$$O_o^x + 2Co_{Co}^{\cdot} \rightleftharpoons V_o^{\cdot\cdot} + 2Co_{Co}^x + \tfrac{1}{2}O_{2(g)} \quad (1)$$

$$O_o^x + 2Co_{Co}^x \rightleftharpoons V_o^{\cdot\cdot} + 2Co_{Co}^{\prime} + \tfrac{1}{2}O_{2(g)} \quad (2)$$

The apparent slopes may be related to the concentration of the multivalent cobalt cation and oxygen vacancies with increasing OPP by external reaction, as shown in Eqs. (1) and (2). The slopes observed from the conductivity measurement cannot, however, be derived by considering the given external reactions at a temperature. As shown in Fig. 6b, Taskin et al. [6] demonstrated that the equilibrium oxygen conent of GBCO is dependent on OPP by the thermogravimetric analysis (X in Fig. 6b represents the oxygen non-stoichiometry). The OPP dependence found by Taskin et al. [6], i.e., a 0.11 power of OPP, is consistent with the dependences observed in the present conductivity measurements. This suggests that the conductivity enhancement with increasing oxygen partial pressure can be directly related to the oxygen content of GBCO. It should be noted, however, that these slopes cannot be predicted simply from Eqs. (1) and (2).

To elucidate potential application of GBCO as a cathode, the ionic conductivity was determined from oxygen permeation measurements. This technique is highly suitable as the electronic conductivity is expected to be several orders of magnitude higher than the oxygen ion conductivity in such a material. The influence of the applied oxygen chemical potential gradient on the oxygen permeability of GBCO is shown in Fig. 7 as a function of temperature. At high temperatures, the oxygen permeation flux increases monotonically with increasing oxygen chemical potential gradient, to yield a maximum of 0.03 $cm^3\,min^{-1}\,cm^{-2}$ under an air/N_2 condition for the 1.14 mm thick GBCO specimen above 1173 K. By constrast, at low-temperature, the oxygen permeation flux exhibits a point of inflection with increasing oxygen potential gradient, which may be related to structural variation with temperature. If bulk diffusion is assumed [13], the oxygen permeation flux across

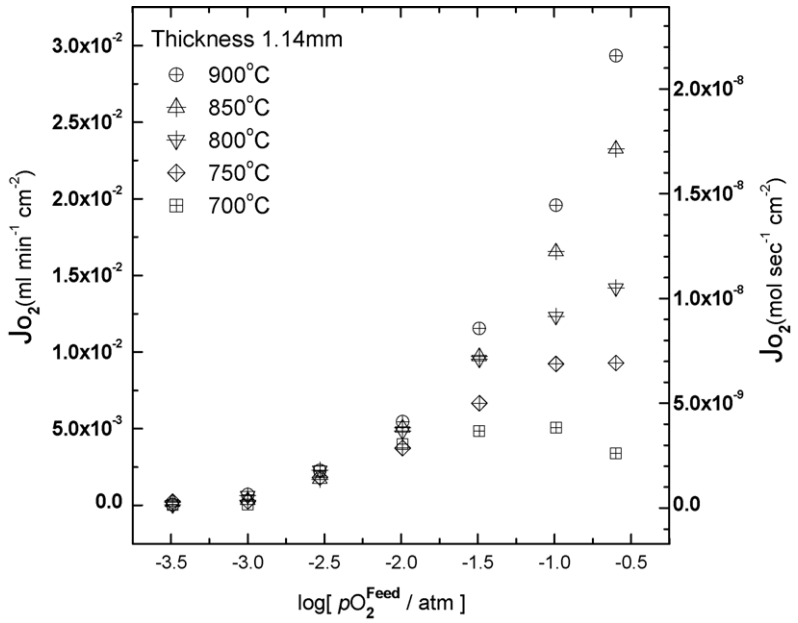

Fig. 7. Oxygen permeation flux as function of oxygen partial pressure (OPP) on feed side at 1173 K for 1.14-mm thick $GdBaCo_2O_{5+\delta}$ specimen.

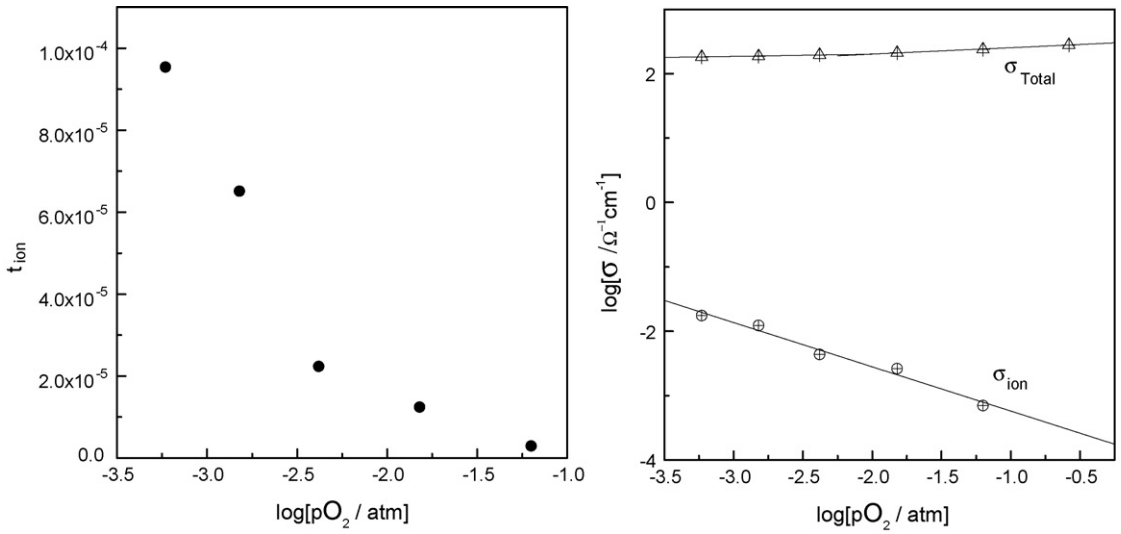

Fig. 8. (a) Transference number of oxygen ion at 1173 K in oxidizing atmosphere and (b) partial oxygen ion conductivity vs. total conductivity as function of oxygen partial pressure (OPP) at 1173 K.

an oxide membrane can be derived from chemical diffusion [14]:

$$J_{O_2} = -\frac{RT}{16LF^2}\int_{\ln P'_{O_2}}^{\ln P''_{O_2}} \frac{\sigma_{el}\sigma_{ion}}{\sigma_{el}+\sigma_{ion}} d\ln P_{O_2} \quad (3)$$

where σ_{el} and σ_{ion} are the electronic and ionic conductivities, respectively; F is the Faraday constant; $d\ln P_{O_2}$ is the oxygen chemical potential gradient across an oxide membrane.

The high total electrical conductivity of GBCO is generally attributed to the hopping of p-type small polarons, associated with the charge disproportionation of Co cations. Because the electronic transference number is believed to be dominant ($\sigma_{ion} \leq \sigma_{el}$), the ionic conductivity may be obtained by differentiation of Eq. (3), i.e.,

$$\sigma_{ion} = \frac{16F^2L}{RT}\left[\frac{\partial J_{O_2}}{\partial \ln P'_{O_2}}\right]_{P''_{O_2}} \quad (4)$$

The data set of different OPP gradients was obtained while the OPP at the reference side was kept constant. In this calculation, the mean slope at a given P'_{O_2} is determined by using the datum at P'_{O_2} and interpolating between its nearest neighbours, as reported previously [15,16]. The calculated ionic conductivity vs. OPP at 1173 K is shown in Fig. 8b. Note that this temperature is above the highest temperature phase transition shown in Fig. 4. The maximum oxygen ion conductivity is around 0.01 S cm^{-1} in nitrogen, which strongly supports the potential of this material for cathode application [17]. The oxygen exponent m, $\sigma_{ion} = P^m_{O_2}$, is assigned a value of −2/3 at 1173 K. The transference number of oxygen, as calculated from the ion/total ratio, is around 10^{-5} at 1173 K, as shown in Fig. 8a.

Fig. 9 gives the typical relaxation profiles of the mean total conductivity, on oxidation and reduction across an identical oxygen activity window, in the exclusively p-type regime of the conductivity shown in Fig. 6a. During the redox reaction, oxygen is incorporated in the GBCO or released from the GBCO. The transient behaviour in the equilibrium process can be best fitted with Fick's second law [18], i.e.,

$$\frac{\sigma(t)-\sigma(0)}{\sigma(\infty)-\sigma(0)} = 1 - \left[\sum_{n=1}^{\infty}\frac{2(\beta_n\tan\beta_n)^2\exp(-(\beta_n^2(\tau-t_0)))}{\beta_n^2(\beta_n^2+(\beta_n\tan\beta_n)^2+\beta_n\tan\beta_n)}\right]^2 \quad (5)$$

where β_n is the positive root of

$$\beta_n\tan\beta_n = L,\ L = \frac{ak}{\tilde{D}} \quad (5a)$$

and σ (0) and σ (∞) denote the equilibrium total conductivity before ($t=0$) and after the relaxation ($t=\infty$), respectively, L is the diffusion length, i.e., half the thickness of the bar-shaped specimen, t is the time, κ is the surface reaction rate constant, and $\tilde{D}$ is the chemical diffusion coefficient. Non-linear-least-squares fitting of the relaxation data in Fig. 9 enable the determination of the chemical diffusion coefficient.

The temperature dependence of the chemical diffusion coefficient and the surface exchange coefficient of GBCO obtained from the d.c. conductivity relaxation in the temperature range of $1073 \leq T(\mathrm{K}) \leq 1323$ and an OPP of 0.21 atm are shown in Fig. 10. The uncertainty level is within the symbol size of the data. Literature-sourced $\tilde{D}$ values [7] are also included in Fig. 10, and the chemical diffusion coefficient values in air at different temperatures are compared with those reported in the literature. As seen from Fig. 10, the present data are an order of magnitude higher than those published in the literature over the complete temperature range, but

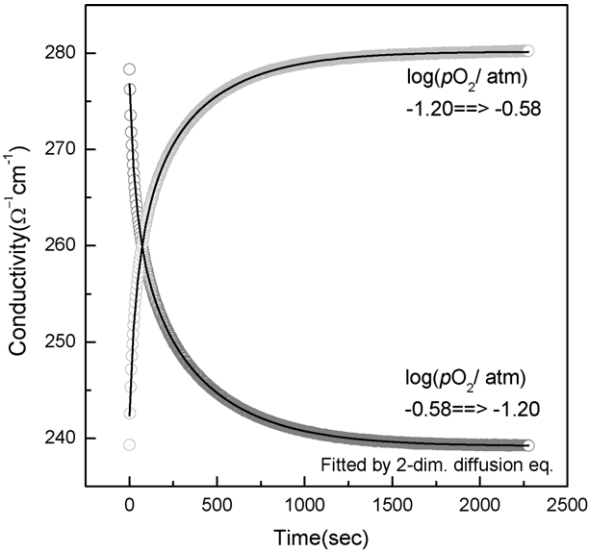

Fig. 9. Typical d.c. conductivity relaxation profiles for $GdBaCo_2O_{5+\delta}$.

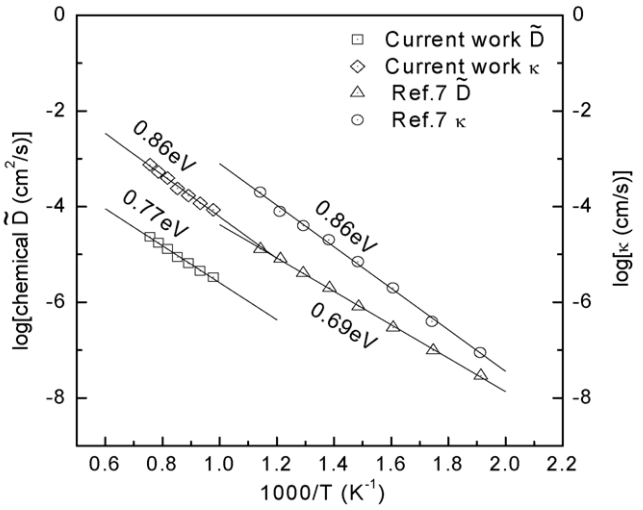

Fig. 10. Temperature dependence of chemical diffusion coefficient and surface exchange coefficient in $GdBaCo_2O_{5+\delta}$.

the activation energy values are similar. This difference may be due to the high temperature phase transition and is under further investigation. Nevertheless, GBCO may be taken as the fast oxygen ion conductor based on the above chemical diffusivity data at these temperature. The $\tilde{D}$ and κ values are best fitted by the following two equations:

$$\tilde{D}\,(\mathrm{cm^2\,s^{-1}}) = 1.88 \times 10^{-2} \exp\left(-\frac{0.77\,\mathrm{eV}}{kT}\right) \quad (6)$$

$$\kappa\,(\mathrm{cm\,s^{-1}}) = 1.37 \times 10^{0} \exp\left(-\frac{0.86\,\mathrm{eV}}{kT}\right) \quad (7)$$

The kinetic values of $\tilde{D}$ and κ are $1.75 \times 10^{-5}\,\mathrm{cm^2\,s^{-1}}$ and $5.3 \times 10^{-4}\,\mathrm{cm\,s^{-1}}$ at 1273 K, respectively. The surface exchange kinetics are of an order of magnitude faster than bulk diffusion.

4. Conclusions

Layered perovskite GBCO powders have been prepared by a conventional solid-state reaction method and their transport properties have been measured as a function of: (a) OPP over the range of $10^{-4} \le pO_2\,(\mathrm{atm}) \le 0.21$ and (b) temperature over the range of $1073 \le T(\mathrm{K}) \le 1323$. Below 1173 K, the average thermal expansion coefficient is about $13 \times 10^{-6}\,\mathrm{K^{-1}}$. The total conductivity increases with increasing temperature below the low-temperature order–disorder transition, thereby indicating semiconductor-type behavior with an activation energy of 0.42 eV. The maximum oxygen permeation flux is $0.03\,\mathrm{cm^3\,min^{-1}\,cm^{-2}}$ under an air/N_2 condition for the 1.14-mm thick GBCO specimen, and the maximum oxygen ion conductivity is around $0.01\,\mathrm{S\,cm^{-1}}$ under nitrogen, which strongly supports the potential for cathode application. The oxygen exponent m, $\sigma_{\mathrm{ion}} = P_{O_2}^{m}$, is assigned a value of $-2/3$ at 1173 K. The chemical diffusion coefficient ($\tilde{D}$) and surface exchange coefficient (κ) values are best fitted by the following two equations:

$$\tilde{D}\,(\mathrm{cm^2\,s^{-1}}) = 1.88 \times 10^{-2} \exp\left(-\frac{0.77\,\mathrm{eV}}{kT}\right),$$

$$\kappa\,(\mathrm{cm\,s^{-1}}) = 1.37 \times 10^{0} \exp\left(-\frac{0.86\,\mathrm{eV}}{kT}\right)$$

Acknowledgments

This research was supported by Basic Science Research Program through the National Research Foundation of Korea(NRF) funded by the Ministry of Education, Science and Technology (R01-2007-000-20586-0).

References

[1] A. Chang, S.J. Skinner, J. Kilner, Solid State Ionics 177 (2006) 2009.
[2] J. Pena-Martinez, A. Tarancon, D. Marrero-Lopez, J.C. Ruiz-Morales, Fuel Cells 8 (2008) 351.
[3] A. Tarancon, A. Morata, G. Dezanneau, S.J. Skinner, J.A. Kilner, S. Estrade, F. Hernandez-Ramirez, F. Peiro, J.R. Morante, J. Power Sources 174 (2007) 255.
[4] A. Tarancon, D. Marrero-Lopez, J. Pena-Martinez, J.C. Ruiz-Morales, P. Nunez, Solid State Ionics 179 (2008) 611.
[5] A. Tarancon, S.J. Skinner, R.J. Chater, F. Hernandez-Ramirez, J.A. Kilner, J. Mater. Chem. 17 (2007) 3175.
[6] A.A. Taskin, A.N. Lavrov, Y. Ando, Appl. Phys. Lett. 86 (2005) 091910.
[7] A.A. Taskin, A.N. Lavrov, Y. Ando, Prog. Solid State Chem. 35 (2007) 481.
[8] M. Yang, Y. Zhong, Z.-K. Liu, Solid State Ionics 178 (2007) 1027.
[9] A. Tarancon, J. Pena-Martinez, D. Marrero-Lopez, A. Morata, J.C. Ruiz-Morales, P. Nunez, Solid State Ionics 179 (2008) 2372.
[10] B. Lin, S. Zhang, L. Lei, H. Ding, X. Liu, J. Gao, G. Meng, J. Power Sources 177 (2008) 330.
[11] C. Frontera, J.L. Garcia-Munoz, A. Llobet, M.A.G. Aranda, Phys. Rev. B 65 (2002) 180405R.
[12] N. Li, Z. Lu, B. Wei, X. Huang, K. Chen, Y. Zhang, W. Su, J. Alloys Compd. 454 (2008) 274.
[13] C. Yang, X. Wu, S. Fang, C. Chen, W. Liu, Mater. Lett. 63 (2009) 1007.
[14] C. Wagner, Z. Phys. Chem. B21 (1933) 25.
[15] S.-J. Song, J.-H. Moon, H.-S. Park, S.E. Dorris, U. Balachandran, Ionics 14 (2008) 37.
[16] S.-J. Song, H.-S. Park, J. Mater. Sci. 42 (15) (2007) 6177.
[17] B.C. Steele, A. Heinzel, Nature 414 (2001) 345.
[18] C.-R. Song, H.-I. Yoo, Solid State Ionics 120 (1999) 141.